Loeb, G. I., & Saroff, H. A. (1964) *Biochemistry 3*, 1819–1826.
Markley, J. L. (1975) *Biochemistry 14*, 3546–3553.
Matthew, J. B., Friend, S. H., Botelho, L. H., Lehman, L. D., Hanania, G. I. H., & Gurd, F. R. N. (1978) *Biochem. Biophys. Res. Commun. 81*, 416–421.
Matthew, J. B., Hanania, G. I. H., & Gurd, F. R. N. (1979a) *Biochemistry 18*, 1919–1928.
Matthew, J. B., Hanania, G. I. H., & Gurd, F. R. N. (1979b) *Biochemistry 18*, 1928–1936.
Matthew, J. B., Friend, S. H., & Gurd, F. R. N. (1981a) *Biochemistry 20*, 571–580.
Matthew, J. B., Friend, S. H., & Gurd, F. R. N. (1981b) *Interactions between Iron and Protein in Oxygen and Electron Transport*, Elsevier/North-Holland, New York.
Matthews, C. R., & Westmorland, D. G. (1973) *Ann. N.Y. Acad. Sci. 222*, 240–253.
Meadows, D. H., Jardetsky, O., Epand, R. M., Ruterjans, H. H., & Scheraga, H. A. (1968) *Proc. Natl. Acad. Sci. U.S.A. 60*, 766–772.
Nagasawa, M., & Holtzer, A. (1964) *J. Am. Chem. Soc. 86*, 531–538.
Niu, C. H., Matsuura, S., Shindo, H., & Cohen, J. S. (1979) *J. Biol. Chem. 254*, 3788–3796.
Richards, F. M. (1982) *Brookhaven Symp. Biol. No. 32*.
Richards, F. M., & Wyckoff, H. W. (1973) *Atlas of Molecular Structure 1. Ribonuclease-S*, Oxford University Press, Ely House, London.
Richarz, R., & Wüthrich, K. (1978) *Biochemistry 17*, 2263–2269.
Saroff, H. A., & Carroll, W. R. (1962) *J. Biol. Chem. 237*, 3384–3387.
Shindo, H., & Cohen, J. S. (1976) *J. Biol. Chem. 251*, 2648–2652.
Shire, S. J., Hanania, G. I. H., & Gurd, F. R. N. (1974) *Biochemistry 13*, 2967–2974.
Tanford, C., & Kirkwood, J. G. (1957) *J. Am. Chem. Soc. 79*, 5333–5339.
Tanford, C., & Roxby, R. (1972) *Biochemistry 11*, 2192–2195.
Wall, F. T., & Berkowitz, J. (1957) *J. Chem. Phys. 26*, 114–122.
Walters, D. E., & Allerhand, A. (1980) *J. Biol. Chem. 255*, 6200–6204.
Wyckoff, H. W., Tsernoglou, D., Hanson, A. W., Knox, J. R., Lee, B., & Richards, F. M. (1970) *J. Biol. Chem. 245*, 305–328.

Torsional Motion and Elasticity of the Deoxyribonucleic Acid Double Helix and Its Nucleosomal Complexes†

I. Hurley, P. Osei-Gyimah, S. Archer, C. P. Scholes, and L. S. Lerman*

ABSTRACT: Torsional thermal oscillations of the DNA double helix within the electron paramagnetic resonance (EPR) time scale (10^{-10}–10^{-3} s) as indicated by a rigid, intercalating probe are much smaller in the spacer segment between nucleosomes in chromatin than in long, free DNA molecules. Still smaller DNA oscillation is indicated in intact nuclei and yet smaller if the nuclei have been treated with glutaraldehyde. The values of EPR measurements are not affected by the loading density of probe. If the probe were capable of substantial oscillations or movement different from that of the helix, those oscillations would be expected to dominate the spectra when movement of the helix is restrained. We conclude that the correlation time for torsional movement of free DNA inferred from EPR spectra is characteristic of the double helix and that there is no significant independent motion of the probe. The correlation time for the DNA double helix in molecules longer than approximately 500 base pairs is close to 30 ns, corresponding to an elastic constant of 1.5×10^{-19} ergs cm for deformation by twisting. The motions observed in chromatin are consistent with a model in which spheres of 50–60-Å radius are connected by simple elastic rods with the length of spacer DNA and the same elastic constant. The spin-labeled ethidium probe has been characterized in detail by nuclear magnetic resonance, infrared, fluorescence, and visible light spectroscopy. The binding equilibria are consistent with the hypothesis that strongly immobilized probe molecules are preferentially bound to spacer DNA.

Previous work in this laboratory (Robinson et al., 1979) has shown the rotational correlation time (τ_r) reported by electron paramagnetic resonance (EPR) spectra of bound spin-labeled ethidium depends upon the size of the DNA molecule with which it is associated. The inferred τ_r was found to increase with increasing DNA length up to a limiting value of 30 ns for double helices 500 base pairs (bp) or longer. These results were seen to be in agreement with the predictions of a model of DNA torsional motion in which the double helix is modeled as a set of coaxial disks linked with torsional springs immersed in a viscous medium (Robinson et al., 1980b). An alternative conjectural explanation for the observed dependence upon length might be that the correlation time increases with increasing length up to a limit imposed by hypothetical independent motion of spin-labeled ethidium relative to the DNA base pairs to which it is bound and does not truly reflect the internal motion of long DNA helices. We will refer to the conjectural independent motion as wobble.

We have now obtained EPR spectra of spin-labeled ethidium bound to DNA in systems in which the motion of each DNA segment is restricted. An approximate upper limit to the extent

† From the Department of Biological Sciences, State University of New York at Albany, Albany, New York 12222 (I.H. and L.S.L.), the Department of Chemistry, Rensselaer Polytechnic Institute, Troy, New York (P.O.-G. and S.A.), the Department of Physics, State University of New York at Albany, Albany, New York 12222, and the Center for Biological Macromolecules, State University of New York at Albany, Albany, New York 12222 (I.H., C.P.S., and L.S.L.). *Received March 16, 1982.* This work was supported by Grants PCM 772558304 and PCM 8111321 from the National Science Foundation.

0006-2960/82/0421-4999$01.25/0

of wobble is established in this paper, much smaller than the motion characterized by the 30-ns correlation time. It is shown that the motional and elastic properties of DNA inferred from our earlier measurements (Robinson et al., 1980a) are essentially correct.

Experimental Procedures

(*1*) *Preparation of Compounds.* Melting points were determined with a Laboratory Devices Melt-temp apparatus and corrected. Infrared spectra were taken on a Perkin-Elmer 621 spectrophotometer. The chemical analyses were performed by Instranal Laboratory, Rensselaer, NY. Analytical results for the elements indicated were within 0.4% of the theoretical values. ^{1}H NMR spectra of the diluter samples (containing 8 mg or less of solute) were obtained with a Bruker WH-90 MHz FT NMR and those of more concentrated samples with a Varian EM 360 60-MHz NMR.

(*a*) *1-Oxy-2,2,5,5-tetramethyl-3-pyrroline-3-carboxylic Acid Chloride.* This compound was prepared according to the method of Rozantzev (1970). An ice-cold stirred suspension of 1-oxy-2,2,5,5-tetramethyl-3-pyrroline-3-carboxylic acid (0.368 g, 0.002 mol) in dry benzene containing excess pyridine was reacted for 1 h with 0.22 mL (0.003 mol) of freshly distilled thionyl chloride added dropwise. The filtrate from the reaction mixture was evaporated in vacuo below 40 °C. The residual oil, 0.41 g, was used without purification.

(*b*) *3-Amino-8-[[(1-oxy-2,2,5,5-tetramethyl-3-pyrrolin-3-yl)carbonyl]amino]-6-phenyl-5-ethylphenanthridinium Chloride (Spin-Labeled Ethidium).* To a mixture of dry ethidium bromide (0.55 g, 0.0014 mol) and 1.2 mL (0.0015 mol) of dry pyridine in 5 mL of dry *N,N*-dimethylformamide (DMF), a solution of the acid chloride (0.41 g, 0.002 mol) in 2 mL of DMF was added dropwise at room temperature. After the mixture was stirred overnight (16 h) the solvent was removed by vacuum distillation. The oily residue was dissolved in 8 mL of 1:1 MeOH–H_2O and refluxed with AgCl 4 h to replace Br^- with Cl^-. The residual red oil obtained by vacuum evaporation of filtrate was chromatographed on preparative TLC plates (silica gel) by using EtOH–$CHCl_3$ (2:1) as the eluant. In order of decreasing R_f, distinguishing color bands of yellow, peach, red, and pink appeared on the plates. The red band, which consisted of the desired compound, was removed from the plate, powdered, and extracted with dry MeOH. The purification procedure using preparative TLC plates was repeated until the red band appeared as a single spot on the TLC plate. The compound was obtained as a solid red residue, 80 mg: mp 267–269 °C; IR (KBr) 3400 (NH-C=O), 1660 cm^{-1} (amide carbonyl). Anal. Calcd for $C_{30}H_{32}O_2N_4Cl\cdot H_2O$: C, 67.46; H, 6.04; N, 10.49. Found: C, 67.83; H, 6.11; N, 10.20.

(*c*) *3-Amino-8-[[(1-hydroxy-2,2,5,5-tetramethyl-3-pyrrolin-3-yl)carbonyl]amino]-6-phenyl-5-ethylphenanthridinium Chloride (Reduced Spin-Labeled Ethidium).* A total of 12.9 mg (2.4×10^{-5} mol) of spin-labeled ethidium in 2 mL of dry DMF was added to 1 mL of butyl mercaptan, and the reaction mixture was stored at room temperature for 5 days. Volatile components were removed by vacuum evaporation. The oily residue was taken up in 0.5 mL of dry Me_2SO and reevaporated. The red solid was dissolved in 0.5 mL of dry MeOH and chromatographed on an analytical TLC plate (silica gel) as before. The principal band was removed, powdered, and extracted with dry methanol. The extract was evaporated to dryness in vacuo: 6 mg of red powder; IR (KBr) 3320 (NOH), 3400 cm^{-1} (NH=CO); NMR δ −1.0–1.6 (m, 13 H), −6.6 (8, 1 H), −8.3–8.8 (m, ~1 H).

(*2*) *Preparation of Biological Materials.* (*a*) *DNA.* High molecular weight chicken erythrocyte DNA (ceDNA) was prepared by a conventional procedure from chicken erythrocytes obtained by cardiac puncture. The A_{200}/A_{260} ratio of solutions of DNA was typically 1.8 in 0.1 M $NaClO_4$–1 mM sodium phosphate, pH 6.8, indicating the absence of complexed proteins. DNA solutions exhibited recoil when swirled and would not penetrate a 60 mg/mL polyacrylamide gel under electrophoresis. DNA was stored in high-salt buffer (2 M NaCl or 2 M $NaClO_4$) and dialyzed against the sample buffer immediately before use. Concentrations of ceDNA solutions were determined by absorbance at 260 nM.

(*b*) *Chicken Erythrocyte Chromatin.* Soluble H_1- and H_5-depleted chromatin was prepared from chicken erythrocytes by the method of Lutter (1978) as modified in Olins' laboratory (A. E. Paton, personal communication). After the multinucleosomal fraction from Sepharose 4B column chromatography was concentrated, the concentrate was dialyzed against 0.2 mM Na_2EDTA–0.1 mM phenylmethanesulfonyl fluoride (PMSF), pH 6.8. Chromatin fragments were sized on a 25 μg/mL polyacrylamide gel after proteinase K digestion. Traces were found of material as small as 3-somes, but the bulk of the DNA ran together as a single band near the gel top, with a mobility 10% of that of monosomal DNA, as expected of DNA from long chromatin fragments (≥10-somes) (Noll et al., 1975). Chromatin samples recovered from solutions used for EPR spectroscopy were redigested and analyzed by gel electrophoresis. A ladder pattern characteristic of extended chromatin was obtained, indicating that the material was well-ordered. Concentrations of chromatin solutions were determined spectrophotometrically.

(*c*) *Chicken Erythrocyte Nuclei.* Chicken erythrocyte nuclei were isolated following the protocol of Olins & Olins (1979), avoiding the use of reagents such as nonionic detergents, high salt, and EDTA, believed to disrupt nuclear structure (Agutter & Richardson, 1980). Phase-contrast micrographs of isolated nuclei confirmed the presence of detailed structures as reported by Olins & Olins (1979). After separation of intact nuclei in a sucrose step gradient and washing with TKM buffer (20 mM Tris-HCl–20 mM KCl–5 mM $MgCl_2$–250 mM sucrose, pH 7) a portion of the nuclear pellet was fixed in glutaraldehyde (3%, in 20 mM sodium cacodylate–5 mM $MgCl_2$–250 mM sucrose, pH 7, for 2 h) and washed 4 times with a Tris-containing buffer (20 mM Tris-HCl–5 mM $MgCl_2$–250 mM sucrose, pH 7) to react with any remaining aldehyde groups. The remaining portion of the nuclei was washed with TKM buffer and stored in a 1:1 TKM buffer–glycerol mixture at −20 °C until used. Unfixed nuclei were always used within 4 days of preparation. Concentrations of DNA in nuclear preparations were estimated spectrophotometrically following lysis and treatment with proteinase K.

(*3*) *Nuclease Digestion.* Freshly prepared chicken erythrocyte nuclei were washed several times with buffer (20 mM Tris-HCl–5 mM $MgCl_2$–250 mM sucrose, pH 7). Most of the pellet was resuspended by pipetting a few times after each wash. The clumped portion of nuclei was discarded. A total of 300 units of micrococcal nuclease (Worthington) was added to the final nuclear suspension (2 mL containing 5.1 mg of DNA), and the suspension was incubated for 1 h at 0 °C. At the end of the hour, 20 μL of a 1 mg/mL solution of spin-labeled ethidium was added, and the nuclei were pelleted by centrifugation. A portion of the moist nuclear pellet was loaded into an EPR tissue cell; the rest was lysed immediately by resuspension and then addition of Na_2EDTA, $NaDodSO_4$, and proteinase K. The course of the room temperature digestion of the sample in the tissue cell was followed by EPR. The DNA in samples of nuclei before and after digestion was analyzed by UV spectroscopy and gel electrophoresis.

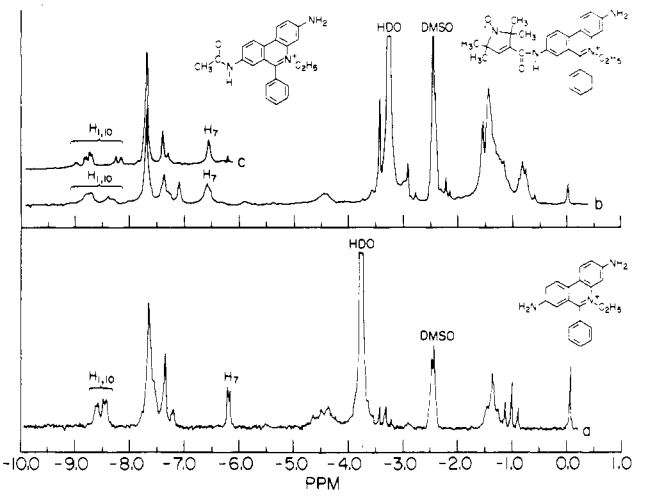

FIGURE 1: Digitized ^1H NMR spectra of (a) ethidium bromide, (b) reduced spin-labeled ethidium chloride, (c) 8-acetylethidium chloride in dimethyl-d_6 sulfoxide (DMSO). Spectrum a was taken by using a 60-MHz conventional NMR; spectra b and c were taken by using a 90-MHz Fourier transform NMR. The large peak at −2.4 ppm is due to proton impurities in Me_2SO. The large peak between −3.0 and −4.0 ppm is due to water.

Results

(*1*) *Characterization of Spin-Labeled Ethidium.* Spectral studies to confirm the structure of spin-labeled ethidium were essential because of the poor yield of product (~10%). Spin-labeled ethidium's NMR spectrum is uninterpretable due to the unpaired electron. Reduction by butyl mercaptan (see Experimental Procedures, section 1c) lowered unpaired spin concentration below detectability by EPR ($<10^{-8}$ M), leaving the phenanthridinium ring unreduced, as indicated by the absence of a large resonance at −4.3 ppm vs. Me_4Si. NMR spectra of reduced spin-labeled ethidium and ethidium are contrasted in Figure 1. Significant differences in the spectrum between ethidium and reduced spin-labeled ethidium indicate that in spin-labeled ethidium a single pyrroline free radical is bonded to the 8 position of phenanthridinium by an amide linkage. These changes are [invoking the assignments of Graves et al. (1977) and Krugh et al. (1975)] as follows: (a) a shift in the position of the H_7 resonance from −6.2 to −6.6 ppm (labeled H_7); (b) an increase in the complexity of the H_1 and H_{10} resonances (labeled H_{1-10}); (c) the appearance of a resonance at −1.46 ppm corresponding to 11 methyl protons. Less significant changes occurring in the positions and intensities of other, poorly resolved, phenanthridinium proton resonances between −7.0 and −7.8 ppm were not analyzed.

The H_7 resonance of ethidium occurs at −6.2 ppm due to ring current effects of the adjacent 6-phenyl substituent, which lies perpendicular to the plane of the phenanthridinium ring (Krugh et al., 1975). The shift of this resonance to lower field in reduced spin-labeled ethidium is due to replacement of the 8-amino group by a more electronegative amide linkage. The same shift occurs when ethidium is converted to 8-acetylethidium (see Figure 1).

The complexity of the H_1–H_{10} resonances of reduced spin-labeled ethidium and their similarity to the corresponding resonances of 8-acetylethidium show addition has occurred only at the 8-amino group. An additional reaction involving the 3-amino group of phenanthridinium should restore the partial electronic symmetry of the H_1 and H_{10} protons and produce a resonance pattern similar to that of ethidium but shifted to lower field. Such an effect has been observed by Graves et al. (1977) in their NMR study of 8-azidoethidium and 3,8-diazidoethidium.

The existence of the resonance at −1.46 ppm in the reduced spin-labeled ethidium NMR spectrum confirms that only one pyrroline ring has been added and suggests the ring has not been significantly degraded during addition. Interpretation of the methyl region of the spectrum is complicated by overlapping resonances at −1.56 ppm and between −0.60 and −0.90 ppm. These resonances were present in the NMR spectrum of ethidium bromide subjected to a mock reduction by butyl mercaptan and may represent nonvolatile impurities in the reducing agent. The resonances of the methyl protons of the ethyl group of spin-labeled ethidium appear between −1.1 and −1.4 ppm as shoulders in the −1.46-ppm resonance, approximately in the same field position as ethidium. The ratio of the sum of the integrated intensities of the pyrroline methyl and ethidium methyl proton resonances to the integrated intensity of the phenyl proton resonance at −7.71 ppm is 5/13 (expected 5/15). Part of the discrepancy is due to unresolved phenanthridinium proton resonances underlying the phenyl proton resonance and contributing to its integrated intensity.

Some other differences between the NMR spectra of ethidium and reduced spin-labeled ethidium have trivial experimental explanations. The shift in the position of the HDO resonance reflects the differing mole fraction of water impurity in the samples. Addition of water to the ethidium sample shifted the HDO resonance further, to −4.6 ppm. The sharp methyl and methylene resonances in the ethidium NMR spectrum are due to the ethanol of the crystallization, as addition of 50 μL of ethanol to an ethidium sample doubled the height of these resonances without perceptibly broadening them.

The EPR evidence completes the characterization of spin-labeled ethidium. At the top of Figure 2 is a 9.5-GHz EPR spectrum of spin-labeled ethidium in aqueous solution. The asymmetric three-line pattern is typical of nitroxide free radicals with rotational correlation times, τ_r, of 100 ps. The separation between lines is 16.2 G. Spin-labeled ethidium solutions purged with nitrogen gas and studied at low modulation levels (≤0.1 G) exhibit resolved superhyperfine structure in the low-field (M = 1) and midfield (M = 0) lines but not in the high-field (M = −1) lines (see Figure 3). Simulations of these spectra indicate that each pattern is composed of signals from 12 equivalent (methyl) protons split by interaction with a 13th (pyrroline) proton. Splittings and line widths appear in the caption of Figure 3. These observations confirm the structure of the pyrroline free radical.

(*2*) *Optical Spectroscopy.* We obtained ultraviolet and visible absorption and fluorescence spectra of spin-labeled ethidium in the presence and absence of a large excess of chicken erythrocyte DNA [r = 0.03 (moles of bound spin-labeled ethidium per moles of DNA base pairs) in 1 mM phosphate buffer]. The visible absorption maximum is shifted from 454–486 nm by binding to DNA, and the extinction coefficient of the maximum decreases from 5000 to 3800. In more concentrated solutions the light yellow-orange color of solvated spin-labeled ethidium changes to a deeper pink on binding to DNA. Both visible maxima occur about 30 nm below the corresponding maxima of ethidium. Other investigators have reported quantitatively similar shifts when primary amino groups of ethidium were modified (Graves et al., 1977; Wakelin & Waring, 1974, 1980).

Our fluorescence spectra were uncorrected for the distribution of source and detector sensitivities. The visible excitation maximum is about 30 nm further toward the blue than ethidium, at 480 nm. The emission maximum of spin-labeled ethidium occurs at the same wavelength as ethidium, 590 nm. Comparison of the fluorescence of bound and unbound spin-

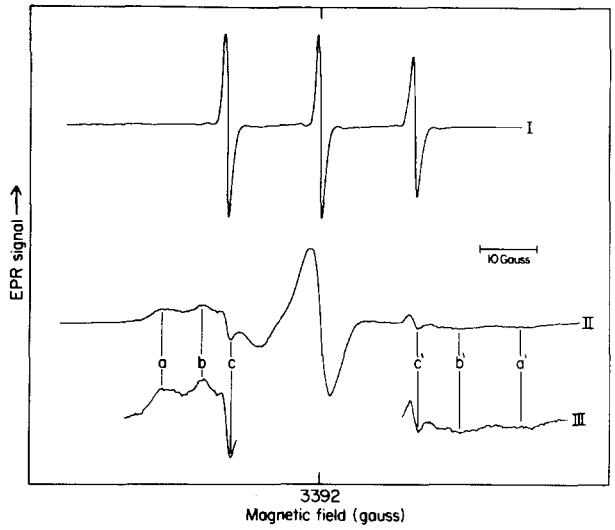

FIGURE 2: 9.5-GHz EPR spectra of spin-labeled ethidium: (I) 2.5 × 10^{-5} M in 10 mM sodium phosphate–1 mM Na_2EDTA (pH 7.6); (II) 4.5 × 10^{-5} M in 0.2 mM Na_2EDTA–0.1 mM phenylmethanesulfonyl fluoride (PMSF) containing ceDNA (r = 0.054). Both spectra were taken at 1.00-G modulation with a Bruker ER-470 EPR spectrometer connected to a Tracor Northern NS-570 digital signal averager. Temperature was maintained at 25 °C with a Bruker VT-1000 temperature controller. This equipment was used to obtain EPR spectra except where indicated. The central field is 3392 G. Spectral features of (II) appear enlarged in (III). Features c and c′ in (II) and (III) arise from unbound spin-labeled ethidium in thermodynamic equilibrium. Features a and a′, the outermost hyperfine features of the most strongly immobilized spin-labeled ethidium, were used to estimate rotational correlation times. Features b and b′ may arise from spin-labeled ethidium that is less strongly immobilized by binding to DNA in a different manner from the probe responsible for features a and a′.

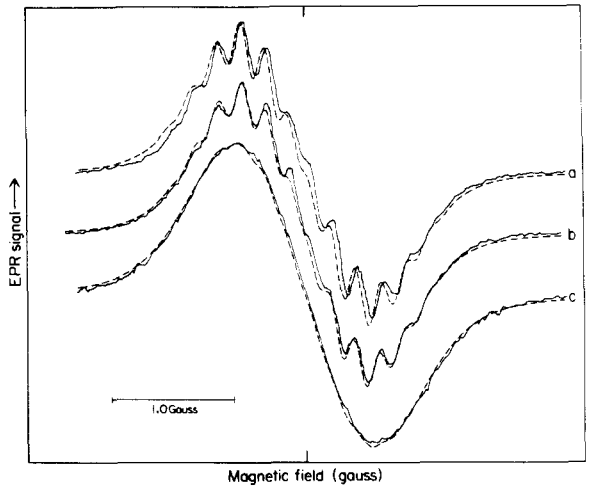

FIGURE 3: Digitized 9.5-GHz EPR spectra of 2.5 × 10^{-5} M unbound spin-labeled ethidium in 10 mM sodium phosphate–1 mM Na_2EDTA saturated with nitrogen gas. (a) Low-field resonance (M = 1), (b) midfield resonance (M = 0), (c) high-field resonance (M = −1). Spectra were taken at 25 °C by using 0.082-G modulation and a Varian E4 EPR spectrometer. The M = 1 and M = 0 exhibit partially resolved superhyperfine structure. The experimental data (solid lines) were modeled by assuming that each is the sum of resonances arising from 13 protons, 12 equivalent methyl protons, and 1 pyrroline ring proton. The best computer-generated least-squares fits (dashed lines) had the following parameters.

	proton splitting (G)			
line	methyl	pyrroline	line width (G)	χ^2
M = 1	0.196	0.512	0.190	0.0011
M = 0	0.192	0.496	0.197	0.0007
M = −1	0.192	0.523	0.287	0.0007

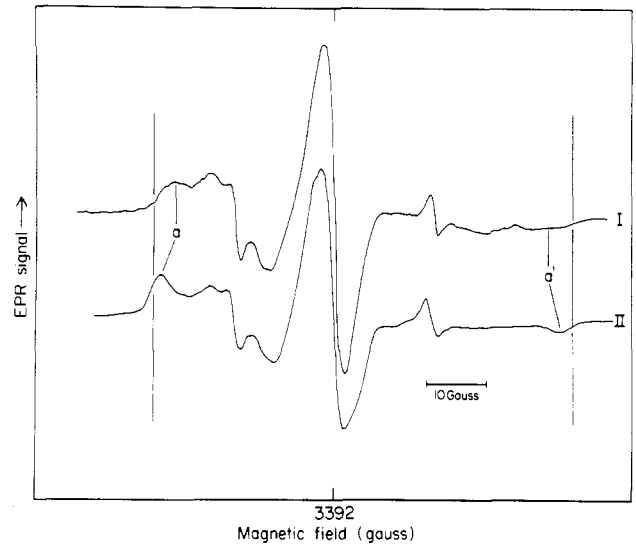

FIGURE 4: 9.5-GHz EPR spectra of spin-labeled ethidium in 0.2 mM Na_2EDTA–0.1 mM PMSF at 25 °C in equilibrium with (I) ceDNA (r = 0.054), (II) soluble chromatin isolated from chicken erythrocytes and stripped of H_1 and H_5 histones (r = 0.013). Spectrum II was obtained by averaging 200 20-s scans. The central field in spectrum II was 3350 G but has been shifted so that the position of the features due to unbound spin-labeled ethidium coincided with those on spectrum I. The vertical lines on the figure represent the rigid limit splitting of spin-labeled ethidium as determined in aqueous sucrose solutions. Positions of the outermost hyperfine features are indicated by features a and a′.

labeled ethidium in the presence of a large excess of DNA indicated that the fluorescence increment on binding was approximately 35, comparable with that of ethidium. The detection limit of fluorescence of spin-labeled ethidium is approximately the same as that of ethidium.

(*3*) *EPR Spectra of Bound Spin-Labeled Ethidium.* The 9.5-GHz EPR spectrum of spin-labeled ethidium in equilibrium with chicken erythrocyte DNA appears at the bottom of Figure 2. Most of the probe binds to DNA, giving a ~70 G wide pattern characteristic of slowly rotating nitroxide spin-labels. A small amount of unbound probe gives rise to the features labeled c and c′ in Figure 2. Two or more binding modes differing in extent of immobilization may contribute independently to the bound spin-labeled ethidium spectrum. The more firmly immobilized ions may give rise to features labeled a and a′ in Figure 2 and less fully immobilized spin-labeled ethidium to features b and b′. Approximately equal numbers of probes appear bound in each mode at low salt, judging from relative sizes of features a and b.

Figure 4 contrasts EPR spectra of spin-labeled ethidium bound to ceDNA and to soluble chromatin at low salt, where chromatin is in its most extended configuration (McGhee & Felsenfeld, 1980). Splitting between features a and a′ is significantly greater in chromatin. Figure 5 shows the dependence of these splittings upon r. A linear regression fit leads to estimates of these splittings in the limit of infinitely small r of 63.9 G for DNA and 66.9 for chromatin. The small decrease in splitting with increasing r does not support the assumption that the helix is stiffened by adding intercalators.

Table I summarizes the dependence of the EPR spectra on sodium ion concentration. As [Na^+] increases from 0.2 to 600 mM there is a relative increase in the height of features c and c′, reflecting a 100-fold decrease in the ratio of bound to free spin-labeled ethidium. Features b and b′ are suppressed more completely than features a and a′, decreasing the signal intensity at 23.7 G below the center of the spectrum compared

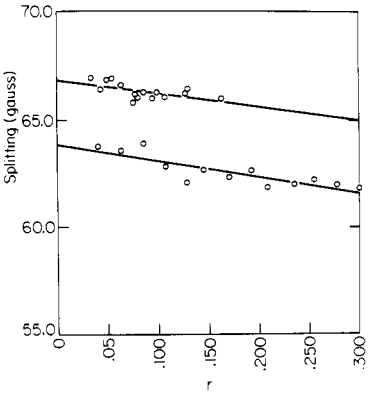

FIGURE 5: Splitting between outermost hyperfine maxima as a function of the probe/DNA base pair ratio. The top line and points refer to spin-labeled ethidium bound to H_1- and H_5-depleted chromatin; the bottom line and points refer to the same probe bound to ceDNA. All spectra taken in 0.2 mM Na_2EDTA–0.1 mM PMSF at 25 °C. Linear least-squares estimates of y intercepts are 66.9 G for chromatin and 63.9 G for DNA.

Table I: Salt Dependence of Spin-Labeled Ethidium EPR Spectra[a]

[Na^+] (mM)	r_1[DNA]/C_{f_1}	h^1/h	splitting (G)	force constant (10^{-19} erg cm)
0.2	120	0.97	63.8	1.4
2.5	58	0.88	63.8	1.4
7.5	21	0.86	64.0	1.5
22	8.5	0.80	64.0	1.5
67	3.1	0.70	64.4	2.0
200	1.2	0.64	65.1	3.2
600	*b*	0.62	65.3	4.0

[a] High molecular weight chicken erythrocyte DNA [(2.6–8.0) × 10^{-4} M) in equilibrium with spin-labeled ethidium ($r \leq 0.06$) in solutions of varying sodium chloride concentration: r_1[DNA]/C_{f_1}, ratio of bound to free spin-labeled ethidium concentration (determined as described in Figure 6); h^1/h, ratio of heights of EPR spectra at 23.7 and 27.1 G downfield of the center (27.1 is the field position of feature a in low salt); splitting, separation of features a and a′ (see Figure 2); force constant, calculated for a long DNA helix of radius 13 Å at 25 °C by using eq 6-11 and the rigid limit given in Figure 9. [b] Not measured, as added sodium chloride significantly reduced cavity Q.

to that at 27.1 G (the field position of feature a in low salt) by 35%. The splitting between features a and a′ also increases, showing that the bound probe moves more slowly as the salt concentration increases.

(*4*) *Binding Equilibria with DNA and Chromatin.* The binding isotherm of spin-labeled ethidium to both DNA and chromatin under identical conditions between r values of 0.01 and 0.20 appear in Figure 6.

Our experimental results were analyzed by using relations developed by Crothers (1968) and McGhee & von Hippel (1974) to describe noncooperative binding of large ligands to a one-dimensional homogeneous lattice. Our DNA data were fitted to the equation (McGhee & von Hippel, 1974)

$$C_{f_1} = \frac{r_1}{K_1(1 - n_1 r_1)}\left(\frac{1 - n_1 r_1}{1 - (n_1 - 1)r_1}\right)^{1-n_1} \quad (1)$$

describing the binding of a ligand of length n_1 base pairs to an indefinitely long helix. The binding constant of the ligand (spin-labeled ethidium) appears as K_1, C_{f_1} corresponds to the concentration of unbound spin-labeled ethidium, and r_1 corresponds to the concentration of bound spin-labeled ethidium in moles bound per mole of DNA base pairs. Chromatin data were fitted to an extension of eq 1 in which a second ligand, of effective binding length n_2 and binding density r_2, is simultaneously in equilibrium (McGhee & von Hippel, 1974):

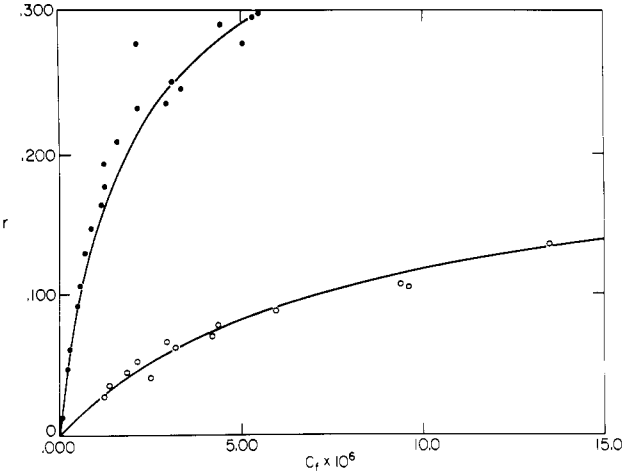

FIGURE 6: Binding of spin-labeled ethidium to DNA and to chromatin: r value (mole ratio of bound spin-labeled ethidium to DNA base pairs) as a function of C_f (concentration of unbound spin-labeled ethidium). C_f was determined by comparing peak-to-peak heights of the M = 1 lines with a set of calibration spectra of 1-oxy-2,2,5,5-tetramethylpyrroline-3-carboxamide (spin amide) taken under the same conditions. The widths of the M = 1 lines of spin-labeled ethidium and spin amide were indistinguishable under the conditions of measurement. Values of r were calculated by subtracting C_f from the total spin-labeled ethidium concentration to estimate bound spin-labeled ethidium. Upper points, ceDNA; lower points, H_1- and H_5-depleted soluble chromatin from chicken erythrocytes. The top curve is a best fit to eq 1 (see the text) by nonlinear least squares. Each parameter was permitted to vary independently. Fitted values are K (equilibrium constant) = 2.4×10^5 and n_1 (effective length of the probe binding site in base pairs) = 2.01. The bottom curve is a best fit to eq 2–4 with values $K = 7.6 \times 10^4$, $n_1 = 1.49$, n_2 (effective length of binding site of core histone complex) = 140 bp (1 bp = 3.4 Å), and r_2 (binding density of core histones complexes in complexes per DNA base pair) = 0.0045. Experiments were performed in 0.2 mM Na_2EDTA–0.1 mM PMSF, pH 6.8, at 25 °C.

$$C_{f_1} = \frac{r_1}{K_1 A}\left(\frac{A}{B}\right)^{1-n_1} \quad (2)$$

$$A = 1 - n_1 r_1 - n_2 r_2 \quad (3)$$

$$B = 1 - (n_1 - 1)r_1 - (n_2 - 1)r_2 \quad (4)$$

The curves represented by solid lines in Figure 6 correspond to least-squares fits to the data determined by a nonlinear parameter search. The binding parameters inferred are given in the caption to that figure.

It is interesting to compare our results with those obtained by others. Paoletti et al. (1977) established, using fluorescence spectroscopy, that ethidium binds in two modes to nuclease solubilized chromatin, one dominating at low r values ($\leq$0.025) and a second, more important one at higher r ($\geq$0.05). Erard et al. (1979) have shown that in first mode ethidium intercalates into spacer DNA and in the second mode ethidium binds cooperatively to core nucleosomes. Saturation of the binding of spin-labeled ethidium to chromatin occurs at a considerably lower r value than that for binding to DNA (see Figure 8). The nonlinear parameter search found best values of n_2 = 140 and r_2 = 0.0045 for chromatin, corresponding to a second ligand 140 bp long bound to DNA at a binding density of 0.0045. This makes 0.63 of the total DNA inaccessible to spin-labeled ethidium. If the DNA in the core nucleosome is inaccessible and DNA in spacer binds probe as

free DNA, the inaccessible fraction of DNA would be 140/205, or 0.68, in agreement with our result within plausible error.

The best value of n_1 in the case of DNA, 2.01, shows binding to nearest neighbors is excluded, as when ethidium intercalates (Waring, 1976). The best value of n_1 in the case of chromatin, 1.49, may indicate that a fraction of spin-labeled ethidium ions is associated with core nucleosomes either internally or by a partial dissociation of DNA from the core nucleosome (Erard et al., 1979) at the r values where saturation becomes noticeable.

The values of K_1 we obtained (2.4×10^5 for DNA, 7.6×10^4 for chromatin) are 1 order of magnitude less than those of ethidium (3×10^6 for DNA, 1×10^6 for chromatin) (Paoletti et al., 1977), in a somewhat higher ionic concentration. Wakelin & Waring (1974, 1980) have found that other 8-modified phenanthridiniums also bind more weakly than ethidium and have attributed the effect to a decreased enthalpy of binding associated with the loss of a primary amino group.

The factor of 3 differences in equilibrium constants between DNA and chromatin observed for both ethidium and spin-labeled ethidium may result from an effect of nucleosomes on the ion atmosphere of spacer in low-salt medium. Brian et al. (1981) have shown the effective electrostatic radius of DNA double helix in dialysis equilibrium with 5 mM sodium ion is approximately 100 Å, half the length of a 60-bp spacer. In our experiments, where the cation concentration is 10-fold lower than in Brian's study, the electrostatic radius of the double helix will be substantially greater, and binding to spacer may be perturbed significantly by the ionic atmosphere of adjacent histones, which will be within the electrostatic radius even in extended chromatin. Electron micrographs of soluble chromatin (Erard et al., 1979) show clustering of nucleosomes, which may have a similar explanation.

Equations 2–4 describing binding were derived by assuming a random distribution of the second ligand on DNA. The core histone complex is distributed in a more uniform, but not completely regular, manner (McGhee & Felsenfeld, 1980). The error this produces in our parameter fit is negligible. At all spin-labeled ethidium concentrations studied, r_1 exceeded r_2, so the majority of the gaps between bound ligands have randomly distributed, bound spin-labeled ethidium ions at each end, as required for the theory developed by McGhee & von Hippel (1974). Only at very low values of r_1 where $r_1 \leq r_2$ must the binding density depend upon the nature of the distribution of the second ligand. In this case a more complex theory will be required to account for this almost regular distribution of core histone complexes.

(5) *EPR Spectra When Bound to Intact Nuclei.* Figure 7 presents EPR spectra of spin-labeled ethidium bound to DNA, to freshly isolated chicken erythrocyte nuclei, and to chicken erythrocyte nuclei fixed with glutaraldehyde. A different buffer (20 mM Tris-HCl–5 mM $MgCl_2$–250 mM sucrose) was used than in the soluble chromatin experiments to maintain stability of condensed chromatin (Olins & Olins, 1979). Its higher viscosity results in a somewhat greater splitting between outermost hyperfine features of the spectrum (64.5 vs. 63.9 G). Since the presence of 5 mM $MgCl_2$ markedly suppresses spin-labeled ethidium binding, DNA measurements were made in concentrated solutions (>40 mg/mL DNA), prepared by centrifugation. Spin-labeled ethidium binding density in these solutions was typically ≤0.002. The splittings between outermost features increase in the order DNA → nuclei → fixed nuclei. To check that the splitting difference was not a result

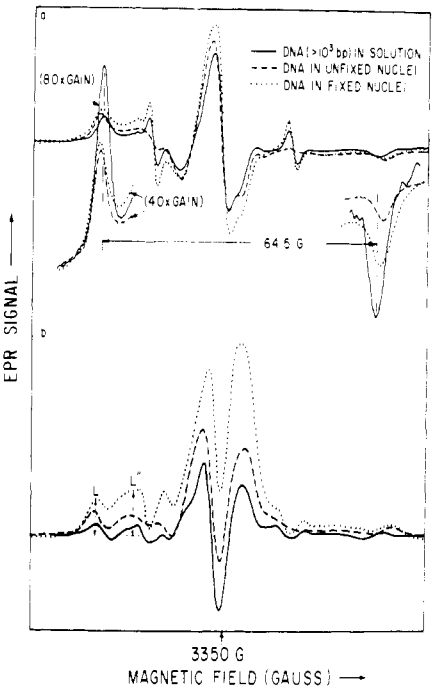

FIGURE 7: (a) Conventional and (b) saturation transfer spectra of spin-labeled ethidium bound to DNA and chicken erythrocyte nuclei. These spectra were taken at 25 °C in a buffer of 20 mM Tris-HCl–5 mM $MgCl_2$–250 mM sucrose pH 7. Up to 250 20-s scans were avgeraged to obtain each spectrum. The r value of each solution was below 0.005. The 100-kHz amplifier of the Bruker ER-470 EPR spectrometer was left on for several days to stabilize. Amplifier phase was found to drift by less than 2° over 5 h after a 24-h warm-up.

of a change in magnetic parameters of bound probe, we determined the effect of increasing sucrose concentration upon freshly prepared nuclei. A 40-fold increase in viscosity caused splitting to increase by approximately 0.5 G, approaching the rigid limit splitting of naked DNA. The splitting difference between fixed and freshly prepared nuclei in linear EPR spectra was not experimentally significant; in saturation transfer (V_2') spectra (see the bottom of Figure 7) the differences are more pronounced. Comparison of these spectra with spin-labeled hemoglobin standards (Thomas et al., 1976) (see Results, section 6) shows that the differences are consistent with increased immobilization in the sequence DNA → nuclei → fixed nuclei.

To determine whether the immobilized spin-labeled ethidium in nuclei is bound principally to DNA, we digested a portion of freshly prepared nuclei with 3 units of micrococcal nuclease/DNA A_{260} unit in the presence of bound spin-labeled ethidium ($r = 0.003$). If binding were to structural proteins or the nuclear cell wall, nuclease digestion should not have changed the EPR spectrum. If the probe binds to spacer DNA, feature a should have decreased and feature c should have increased in the latter part of the digestion, when available binding sites become few relative to spin-labeled ethidium ions. Gel electrophoresis of samples taken during digestion indicated that almost all nuclear DNA was digested to small fragments after 45 min, while 1–10% of total DNA resisted nuclease action for more than 24 h. This fraction may represent nuclei trapped in the debris of the digestion of its neighbors or within erythrocyte cell membranes or DNA protected by association with the nuclear protein matrix or nuclear membrane, as has been noted by others (Agutter & Richardson, 1980). Figure 8 contains EPR spectra taken during the digestion. After 80 min (35 min at 0 °C, 45 min at room temperature) the intensity of feature a decreases,

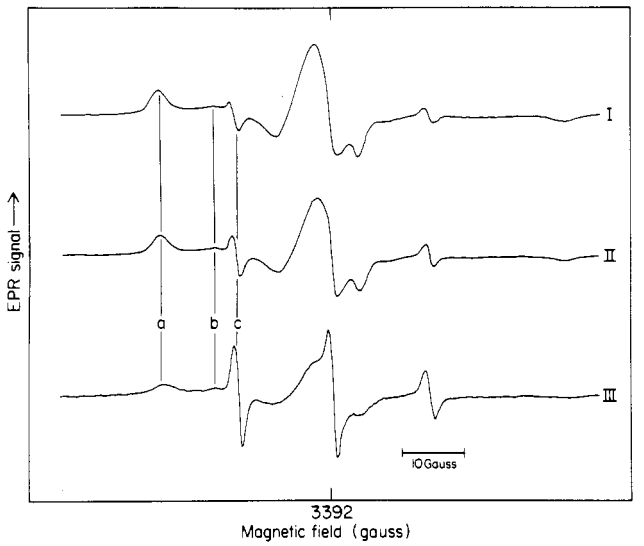

FIGURE 8: Effect of digestion of chicken erythrocyte nuclei with micrococcal nuclease (3 nuclease units/DNA A_{260} units) at room temperature upon the spectra of spin-labeled ethidium. Spectrum I was taken with no nuclease present (sample not digested). Spectrum II was taken 80 min after adding nuclease. Spectrum III was taken 6 h after adding nuclease. The digestion buffer was 20 mM Tris-HCl–5 mM $MgCl_2$, 2.0 $CaCl_2$–250 mM sucrose. Digestion was carried out in an EPR tissue cell kept in a condensation chamber at room temperature between spectra. Total DNA content of digested sample was 0.86 mg; that of the sample not digested was 0.99 mg. The same amount of spin-labeled ethidium was added to both samples. Amplifier gains at which spectra were taken were, for spectrum I, 1.2×10^3, for spectrum II, 2.0×10^3, and, for spectrum III, 3.2×10^3. Features a, b, and c are as described in Figure 2.

indicating decreased bound probe, while the intensity of feature c remains approximately constant (note the change of gain in Figure 8), showing that the probe is bound primarily to the DNA in the nuclei rather than to cell walls or structural proteins. The decrease in total spin-label concentration, bound and unbound, during digestion is probably due to reduction of unpaired spin by nuclease, as no decrease was noted where nuclease was absent. At termination of digestion feature a was 10% of its initial value, shifted 0.6 G toward the center of the spectrum, and broadened by one-quarter, indicating a wider distribution of mobilities for the strongly immobilized probe. Corresponding results have been obtained for the intercalator, ethidium azide, in a different type of experiment (Graves et al., 1981).

(6) What Are the Rotational Correlation Times Reported by Spin-Labeled Ethidium Bound to DNA, to Soluble Chromatin, and to Chromatin in Nuclei? Three semiempirical methods have been developed to estimate rotational correlation times of slowly tumbling nitroxide radicals from EPR spectral features: the ΔS method (McCalley et al., 1972; Goldman et al., 1972), the two-frequency method (Hyde & Rao, 1980), and a lifetime broadening method (Mason & Freed, 1974). We have relied mainly on the ΔS method to estimate τ_r and have checked results in a few instances by the two-frequency method.

The rigid limit splitting needed to apply the ΔS method was determined by extrapolating a plot of splitting as a function of viscosity^{-1} to the limit of infinite viscosity (see Figure 9). This procedure minimized perturbation of magnetic properties by immobilization and for that reason is preferable to freezing in liquid N_2 or ammonium sulfate precipitation (Johnson, 1979). Our experimental data were fitted to

$$\eta^{-1} = 2C(A_{zz}^0 - A_{zz})^b \quad (5)$$

where η is the solution viscosity, $2A_{zz}$ is the experimental

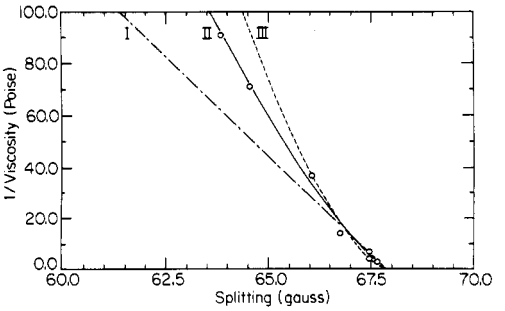

FIGURE 9: Sucrose dependence of splitting between outermost hyperfine maxima of 9.5-GHz EPR spectra of spin-labeled ethidium bound to short DNA fragments. The spin-labeled ethidium concentration was 2.4×10^{-6} M. Sonicated, fractionally precipitated chicken erythrocyte DNA of average length 1200 bp was used in this experiment ($r = 0.07$). Measurements were made at 24 °C. Viscosities were inferred from measured solution densities. At least 60 50-s scans were averaged to produce each spectrum. The central line, II, is a best fit to eq 5 by using a nonlinear least-squares program. The extrapolated value of rigid limit splitting, $2A_{zz}^0$, was 67.9 G. The value of b obtained was 1.28 and c was 15.3. The lines I and III represent the same function plotted with b's of 1.0 and 1.5. The value of b obtained indicates that probes relax by a Brownian diffusion process.

Table II: Rotational Correlation Times by EPR at 25 °C

substrate	ΔS Method buffer[a]	splitting (G)	τ_r (ns)
DNA	Na_2EDTA	63.9	30
DNA	Mg^{2+}	64.5	40
nuclease-solubilized chromatin	Na_2EDTA	66.9	200
freshly isolated nuclei	Mg^{2+}	66.9	200
nuclei fixed with glutaraldehyde	Mg^{2+}	67.4	>400

substrate	buffer[a]	Two-Frequency Method ½ splitting (9.5 GHz) (G)	splitting at (35 GHz) (G)	τ_r (ns)
DNA	Mg^{2+}	32.5	31.3	30
DNA	K^+	32.2	31.1	40

substrate	Saturation Transfer EPR buffer	L''/L	τ_r (ns)
DNA	Mg^{2+}	0.59	<100
freshly isolated nuclei	Mg^{2+}	0.81	1×10^5
nuclei fixed with glutaraldehyde	Mg^{2+}	1.24	$>1 \times 10^6$

[a] Buffer: Mg^{2+} = 5 mM $MgCl_2$–20 mM Tris-HCl–250 mM sucrose, pH 7.5; K^+ = 20 mM KCl–20 mM Tris-HCl–250 mM sucrose, pH 7.5; Na_2EDTA = 0.2 mM Na_2EDTA–0.1 mM PMSF, pH 6.8.

splitting at that viscosity, $2A_{zz}^0$ is the rigid limit splitting, and C and b are parameters determined by the fitting process. This equation was derived from the empirical relation between splitting and rotational correlation time of Freed (1976) assuming a Stokes–Einstein relation between τ_r and viscosity. This assumption is not true for the coupled disk model of DNA rotational motion (Robinson et al., 1980a), except in the limit of long times and small oscillation amplitudes. It is acceptable in this case because of the high viscosities of these sucrose solutions. Our fitted value of b, 1.28, falls in the range Freed (1976) obtained for Brownian rotational diffusion and is significantly different from values obtained where reorientation occurs by a jump or free diffusion process. This is evidence for the validity of the assumption of Brownian diffusion made in deriving the coupled disk model of DNA motion. The value of b also determined which of Freed's calibration curves was

appropriate to relate the measured splittings to the rotational correlation times presented in Table II.

These correlation times are not all equally reliable. Those of DNA, 30–40 ns, lie within the time scale in which the ΔS method is normally believed valid. At longer times, such as the 200 ns τ_r apparently reported by probes bound to chromatin and freshly prepared nuclei, the splitting between hyperfine extrema is known to depend upon details of probe motion (Freed, 1976). The values of τ_r for movement around the helix axis in nuclei and chromatin may be as much as 1 order of magnitude longer than that reported here. The similarity of the correlation times characterizing chromatin and nuclei probably reflects the imprecision involved in measuring splittings rather than any real agreement. Both splittings are, however, experimentally distinguishable from the rigid limit and show that DNA of fresh nuclei and chromatin carrying bound probe have some residual rotational mobility. This is not true for fixed nuclei, where the splitting is not distinguishable from the rigid limit and no estimate of motional freedom can be inferred.

The two-frequency method was applied to spectra of spin-labeled ethidium bound to concentrated DNA (>40 mg/mL) at low r values ($\leq$0.002) in viscous buffers (e.g., 20 mM Tris-HCl–5 mM $MgCl_2$–250 mM sucrose) to check our values of τ_r. We used a Varian V-4500 EPR spectrometer fitted with a V 45G1 35-GHz microwave bridge to obtain spectra at 35 GHz. Since the two-frequency method does not involve determining rigid limit splitting, the reasonable agreement between the value of τ_r obtained by the ΔS and two-frequency methods shows A_{zz}^0 must not be substantially in error (the results of this determination appear in Table II).

Measurement of the relative heights of features of the second harmonic out of phase absorption passage saturation transfer (V_2') spectra was applied to provide a more sensitive estimate of correlation times in nuclei. Thomas et al. (1976) prepared a calibration curve relating these heights in a set of spin-labeled hemoglobin standard spectra that rotate isotropically to their τ_r's at varying viscosity/temperature ratios. Use of these curves where the rotational motion is anisotropic is fraught with difficulty (McGaffney, 1979; Hyde & Dalton, 1979; Robinson & Dalton, 1980). Comparison of our spectra with spectra of anisotropically moving spin-labels suggests spin-labeled ethidium bound to DNA and nuclei is moving anisotropically (McGaffney, 1979; Hyde & Dalton, 1979). The theoretical implications of these difficulties have not been completely worked out. Of the three measurements that could be made to estimate τ_r, those made further away from the central feature are less perturbed by motional anisotropies (Robinson & Dalton, 1980), so we have used low-field features L and L'' to obtain the correlation times in Table II. The DNA correlation time obtained is lower than expected from linear EPR and our DNA motion model (see Discussion, section 2) and may be in error due to a contribution to the height L'' from the nearby resonance of partially immobilized spin probe. This interference is less significant in the other spectra, as the absolute height L'' is greater.

Comparison of the τ_r's from freshly prepared and fixed nuclei indicates strong immobilization of the probe in nuclei, of the order of a 100-fold increase in τ_r. Fixing nuclei increases immobilization by another factor of 10. The measurement with fixed nuclei lies at the limit of the longest times accessible by the saturation transfer and must represent only an upper limit to the mobility of DNA in fixed nuclei. These results are in reasonable agreement with those obtained by the ΔS method when allowance is made for T_e dependence (see Discussion, section 2) and the approximations involved in using the ΔS method to determine long τ_r's.

Discussion

(*1*) *What Is the Nature of the Binding of Spin-Labeled Ethidium to DNA, Chromatin, and Nuclei*? The overall EPR spectrum appears to be a sum of spectra due to probes in two binding modes differing in rate of motion (see Figure 2). The overall binding affinity of spin-labeled ethidium is comparable with that of acridine spin-labels (Robinson et al., 1980a). Roughly equal amounts of probe are bound in each of two modes at low salt, and the fraction of the mode showing more rapid motion decreases as salt increases (see Results, section 3). Our study of DNA motions and the evidence for the close coupling of probe to the helix, presented in this paper, concerns the properties of this first mode only. These conclusions are not affected by the presence of an additonal independent binding mode that may allow greater motion.

The following arguments support identification of the tightly coupled binding mode with intercalation. The amide link between the pyrroline ring and the phenanthridinium has the same stereochemistry as intercalating, spin-labeled derivatives of 6-aminoacridine (Robinson et al., 1980a). Space-filling models show no obstacle to intercalated binding, and the fit of probe into an opened helix appears snug, as would be expected with no wobble. The bathochromic shift and decrease in extinction coefficient upon binding to DNA agree closely with those of ethidium and other 8-substituted ethidium derivatives when these intercalate (Wakelin & Waring, 1974, 1980). The fluorescence emission spectrum and observed fluorescence enhancement of bound spin-labeled ethidium resembles those of ethidium (see Results, section 2). The binding isotherm shows the ratio of total binding sites and the ratios of binding constants between chromatin and free DNA are similar to those of ethidium (Figure 6).

We may speculate, without evidence, that the second mode represents some form of external attachment without close contact at a sufficiently large number of points to prevent rocking.

Our nuclease digestion study (see Results, section 5) shows that spin-labeled ethidium binds preferentially to the DNA of chicken erythrocyte nuclei rather than any structural proteins that may be present. Combined with the known lack of metabolic activity in chicken erythrocytes (implying the absence of RNAs) and our chromatin binding isotherm, this suggests that the majority of strongly immobilized probe is bound to the spacer regions of the chromatin in nuclei. The evidence available is not sufficient to decide whether this chromatin is in the form of condensed 25 nM fibers or is a small subset in a more extended form. Liberation of probe by nuclease digestion shows that it is not bound preferentially to DNA associated with the nuclear protein matrix.

(*2*) *What Is the Motion of DNA Reported by Spin-Labeled Ethidium*? Two types of motion might be followed by spin-labeled ethidium—movements of the whole DNA molecule or internal motions on a much smaller scale. The calculated rate of overall tumbling or axial rotation of short rigid rods of one persistence length (Barkley & Zimm, 1979) indicates rotational correlation many times larger than the 30 ns we observe. Our value of 30 ns would correspond to rigid rod rotation of 60 or so base pairs, but it is hard to conceive of a mechanism for the swivels that could connect such 60-bp segments to make a long DNA molecule (Robinson et al., 1980a). A more plausible model of DNA motion in which the base pairs are represented by disks connected by coaxial torsional springs (Robinson et al., 1979) is illustrated in Figure

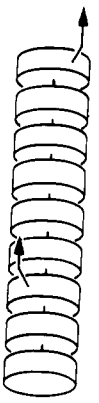

FIGURE 10: Physical model of DNA torsional motion. The base pairs are represented in this model by disks connected by torsional springs. The random thermal rotational oscillations of each disk are coupled to its immediate neighbors. The intercalated spin-labeled probe is represented by a disk with a pointer at one side. The spin-labeled probe is assumed to act as a normal base pair.

10. The disks with arrows attached represent the reporter, intercalated spin-labeled ethidium. These are hypothesized to act as typical disks of the stack. Overall motion is treated as a set of random normal mode oscillations. When the coupled differential equations representing this system are solved under circular boundary conditions, the following equations relating the physical properties of DNA to the corresponding rotational correlation time are obtained (Robinson et al., 1980a,b):

$$\tau_0 = 3.4\pi R^2\eta/(kT) \tag{6}$$

$$g = 2t/(A^2\tau_0) \tag{7}$$

$$\Omega(g,N) = \frac{1}{N}\sum_{j=1}^{N}\frac{1-\exp[-g\sin^2(\pi j/N)]}{g\sin^2(\pi j/N)} \tag{8}$$

$$\tau_f = \int_0^\infty e^{-t/T_e}e^{-\Omega(g,N)t/\tau_0}\,dt \tag{9}$$

$$\tau_r^{-1} = \tau_f^{-1} - T_e^{-1} \tag{10}$$

$$A^2 = kT/f \tag{11}$$

The parameters characterizing individual disk motion are its radius, R, the harmonic force constant of the torsional spring linking two discs, f, the absolute temperature, T, and Boltzmann's constant, k. The factor 3.4 appears as the thickness of a single disk or base pair, 3.4 Å. N is the number of disks in the system and limits the number of normal modes of vibration. A is the root mean square oscillation amplitude of a single disk. T_e represents the intrinsic relaxation time of the probe. The variable of integration, t, is time. In practice, evaluation of the integral is not carried to infinity. Contributions from $t > 10T_e$ are negligible. This model is formally equivalent to one developed independently by Barkley & Zimm (1979) and Shore & Zwanzig (1975) to interpret the results of relaxation experiments. The model above considers only torsional (twisting) motion; it does not consider flexure (bending). Applying this model to interpret our experimental DNA τ_r of 30 ns, we obtain a root mean square torsional oscillation amplitude of each disk of 6° at 25 °C and a harmonic torsional force constant for DNA of 1.5×10^{-19} erg cm. This result is in agreement with our previous determination (Robinson et al., 1979, 1980a).

This force constant is also in good agreement with values deduced by others: the fluorescence depolarization measurements of Millar et al. (1980), Barkley & Zimm's (1979) treatment of Wahl et al.'s (1970) fluorescence data, the linking number determinations of Pulleyblank et al. (1975), and Depew & Wang (1975). In addition, values decided from computer simulations of Levitt (1978) and Miller (1979) are in order of magnitude agreement with this result.

Two features of this model deserve further explication. First, the model proposes that observed τ_r depends upon the characteristic rate constant (T_e) for spin relaxation. In eq 9 T_e acts to pick out terms in the normal mode expansion of $\Omega(g,N)$ (eq 8) that will make the largest contributions to τ_f and ultimately to τ_r (eq 10). For conventional EPR $T_e = T_2$, while for passage saturation transfer EPR $T_e = T_1$. Nitroxide free radicals typically exhibit $T_1 = 300T_2$ (Hyde & Dalton, 1979). Therefore, saturation transfer measurements are maximally sensitive to normal modes of oscillation of greater wavelength than in linear EPR. The τ_r predicted to be observed in a passage saturation transfer experiment on the basis of our linear EPR results, the theory above, and the known relationship between T_1 and T_2 is approximately 100 ns. This is longer than our experimental τ_r (<100 ns). Plausible reasons for the discrepancy have been discussed in section 6 under Results.

Second, the model predicts that τ_r should depend upon DNA length for short double helices but be independent of length beyond a characteristic length depending upon T and f. For DNA shorter than the characteristic length orientations of disks at opposite ends of the stack are partially correlated with each other as the torsional force constant is high enough and the springs are stiff enough to couple motions involving opposite ends. Rotational relaxation for very short lengths occurs principally through rigid rod rotation about its long axis. The rotational correlation time for a rigid rod is directly proportional to its length, and so τ_r will be a linear function of length for short helices. Well above that characteristic length rigid rod rotation is sufficiently slow that normal mode oscillations (as weighted by T_e) dominate relaxation. Increasing the length of the helix, though it adds longer wavelength normal modes, does not change τ_r, as these normal modes decay with times much longer than T_e and so make little additional contribution to τ_f (eq 9). In DNA helices of intermediate length (~90–300 bp for circular DNA at 25 °C (Robinson et al., 1979)] τ_r is a complex function of length with both internal oscillation and rigid rod rotation contributing. We have experimentally confirmed that the length dependence exists, though agreement with theory is not completely satisfactory, possibly because of neglect of bending motions (Robinson et al., 1980b) or because of the polydispersity of the experimental material.

This model might be adapted to accommodate a local stiffening of the double helix in the vicinity of the intercalator. Such stiffening can be expected in view of the distortions introduced into the backbone to accommodate an intercalator. This would involve introducing a larger force constant for the springs immediately adjacent to the reporter disk. It is unlikely an exact solution of this new model would differ significantly from our present one. We know reporter disk relaxation involves concerted motion of stacks much longer than three that would be linked by stiffer springs in the new model (Robinson et al., 1980a). Averaged over 200 or more base pairs, the perturbation from a few stiffer springs should be negligible. Further, at low binding density of intercalator, the average force constant should approach that in the absence of intercalator. The experimental very slight dependence of splitting on binding density agrees with this line of argument (see Figure 5). Measurements at very high loading where the intercalators

are likely to be sufficiently close for relaxation to occur by spin exchange are not expected to be useful.

(3) *Does the Spin-Labeled Ethidium Wobble When Bound to DNA?* In the experiments with chromatin and nuclei we have examined the effect of a constraint on the helix motion that does not exert any direct effect on the probe. Increase in the viscosity of the medium is not equivalent, since the probes are in contact with the medium and are subjected to viscous drag. An alternating pattern of nucleosomes and spacer DNA in extended chromatin can be regarded as a double helix loaded at intervals with spherical dampers; movement of spacer DNA is constrained by the lower mobility of the nucleosomes while the probe retains the same local environment as in normal DNA. If the motion reported by bound spin-labeled ethidium were attributable to wobble, the observed correlation times would be the same for naked DNA and chromatin.

The results reported in sections 3 and 4 under Results confirm that spin-labeled ethidium is bound preferentially to spacer DNA and that the probe motion is slower when bound to chromatin. We conclude that the probe does not wobble significantly when bound to DNA. The results reported in section 5 under Results involving the condensed chromatin of nuclei indicate the wobble rate is much smaller than spacer motion in chromatin.

A quantitative estimate of the maximum contribution of wobble to DNA motion can be made if we assume that the residual motion reported by probe bound to fixed nuclei is isotropic and represents wobble. Then

$$\tau_r^{-1}(\text{true}) = \tau_r^{-1}(\text{measured}) - \tau_r^{-1}(\text{fixed nuclei}) \quad (12)$$

Using the results in Table II, we calculated that the maximum contribution of wobble is 0.009% to the observed overall motion of high molecular weight DNA, 0.07% to the observed motion of soluble chromatin, and approximately 20% to the motion of condensed chromatin in nuclei.

(4) *Salt Dependence of DNA Torsional Flexibility.* We observe a monotonic increase in splitting between EPR hyperfine extrema with increasing salt (Results, section 3). Using the rigid limit reported in Figure 9 and eq 6–11, we calculate a corresponding 3-fold increase in DNA torsional stiffness between 0.2 and 600 mM Na^+ (see Table I). There are at least two possible explanations for this phenomenon. Torsional flexibility may be sensitive to base composition, and increasing salt could increase the preference of probes for binding sites in relatively stiff regions. Alternatively, a slight structural extension of DNA due to additional intrahelical electrostatic repulsion in low salt may somewhat disengage short-range barriers to rotation.

(5) *A Model for Chromatin Motion.* An extension of our motional model to chromatin would introduce a sphere or disk of appropriate dimensions to represent the nucleosome core, with the spacer DNA being modeled as a string of 60 or so coupled disks as before. Solution of the dynamic equations describing this model involves considerable difficulties; for example, the motion of the disks in the spacer region will depend upon their distance from the nearest nucleosome core, and the motion reported by the probe will have to be averaged over all binding sites. We have therefore postponed our attack on this problem, especially as a more tractable model promises to be at least approximately correct.

This second model of chromatin involves core nucleosomes as spheres with a radius between 50 and 60 Å and spacer DNA as a uniformly deformable rod of negligible cross section with the torsional force constant of DNA (1.5×10^{-19} erg cm). Neglect of friction between spacer DNA and solvent should not introduce a significant error as frictional drag depends upon the square of the radius of the rotating surface, and drag on nucleosome cores should dominate. The rotational correlation time of the isolated nucleosome core for motion about one axis is taken to be

$$\tau_0 = 2\pi R^3 \eta/(kT) \quad (13)$$

Solving of this equation with eq 7–11 permited us to estimate the torsional correlation times for core nucleosomes. The results of these calculations appear in Table III for T_e characteristic of linear EPR in the limit of very long chromatin. Notice that the expected τ_r depends strongly upon the core nucleosome radius (τ_r = 199 ns for 50 Å, but τ_r = 325 ns for 60 Å) and less so upon the length of spacer DNA (τ_r = 199 ns for 60 bp and 272 for 15 bp) and the DNA torsional force constant (τ_r = 199 ns for force constant = 1.5×10^{-19} erg cm, and τ_r = 261 for force constant = 4.1×10^{-19} erg cm). Most significantly, in all cases, τ_r is increased by coupling the nucleosomes together with the spacer DNA. Motion of chryromatin must therefore involve concerted motions of more than a single core nucleosome.

Table III: Calculated Chromatin Dynamics Using the Torsional Bead Model

force constant (10^{-19} erg cm)	spacer DNA (bp)	core nucleosome radius (Å)	τ_0 (ns)	τ_r (ns)
1.5	60	50	170	199
1.5	60	60	293	325
4.1	60	50	170	261
1.5	15	50	170	272

[a] τ_0 = predicted rotational correlation for a single nucleosome rotating about a single axis at 25 °C in a medium of 1 cP. [b] τ_r = predicted rotational correlation time for an indefinitely long chromatin fragment at 25 °C in a medium of 1 cP. Effects of flexure are neglected and circular boundary conditions are assumed. The values of the DNA force constant used are ours (Robinson et al., 1979) (1.5×10^{-19} erg cm) and that of Barkley & Zimm (1979) (4.1×10^{-19} erg cm).

The motion we have probed experimentally, of spin-labeled ethidium bound in the spacer region, must be partially correlated with the motion of the nearer core nucleosome, as their average separation is 15 bp, a length short enough that the motion at the nucleosome would be quite closely coupled according to our estimate of torsional stiffness. The τ_r the spin-labeled ethidium probes report should be shorter than those in Table III, as there will be extra modes of oscillation with nucleosomes motionless (with an integral number of half-wavelengths in the spacer region) contributing to the rotational relaxation of probes but not of core nucleosomes. Or experimental τ_r of spin-labeled ethidium bound to soluble chromatin (~200 ns, Table II) appears to be in good agreement with this approximate calculation.

We think that the rotational motion is so small in nuclei because the chromatin is organized into 25 nM fibers (Olins & Olins, 1979) in which the nucleosomes are compacted into a helical array and no longer able to move independently. While it is not yet possible to construct physical models to describe rotational relaxation of these condensed systems, the effect of glutaraldehyde cross-linking upon motion agrees with the supposition that concerted motions involving multiple nucleosomes are involved.

Added in Proof

Recent improvements in theory (B. H. Robinson, personal communication) suggest that small values of τ_r inferred from

saturation transfer spectra may be underestimated by the relations used here. Although the saturation transfer correlation time for free DNA given in Table II would be revised upward, the ratio between the values of τ_r in nuclei and free DNA would remain very large, and the ratio between fixed and unfixed nuclei would not be changed significantly.

References

Agutter, P. S., & Richardson, J. C. W. (1980) *J. Cell Sci. 44*, 395.

Barkley, M. D., & Zimm, B. H. (1979) *J. Chem. Phys. 102*, 2991.

Brian, A. A., Frisch, H. L., & Lerman, L. S. (1981) *Biopolymers 20*, 1305.

Crothers, D. M. (1968) *Biopolymers 6*, 575.

Depew, R. E., & Wang, J. C. (1975) *Proc. Natl. Acad. Sci. U.S.A. 72*, 4275.

Erard, M., Das, G. C., deMurcia, G., Mazer, A., Pouyet, J., Champagne, M., & Daune, M. (1979) *Nucleic Acids Res. 6*, 3231.

Freed, H. H. (1976) in *Spin Labelling I* (Berlinger, L. S., Ed.) Academic Press, New York.

Goldman, S. A., Bruno, G. C., & Freed, J. H. (1972) *J. Phys. Chem. 76*, 1858.

Graves, D. E., Yielding, L. W., Watkins, C. L., & Yielding, K. L. (1977) *Biochim. Biophys. Acta 479*, 98.

Graves, D. E., Watkins, C. L., & Yielding, L. W. (1981) *Biochemistry 20*, 1887.

Hyde, J. S., & Dalton, L. R. (1979) in *Spin Labelling II* (Berliner, L. S., Ed.) Academic Press, New York.

Hyde, J. S., & Rao, K. V. S. (1980) *J. Magn. Reson. 38*, 313.

Johnson, M. E. (1979) *FEBS Lett. 97*, 363.

Krugh, T. B., Wittlin, F. N., & Cramer, S. P. (1975) *Biopolymers 14*, 197.

Levitt, M. (1978) *Proc. Natl. Acad. Sci. U.S.A. 75*, 640.

Lutter, L. C. (1978) *J. Mol. Biol. 124*, 139.

Mason, R. P., & Freed, J. H. (1974) *J. Phys. Chem. 78*, 1321.

McCalley, R. C., Shimshick, E. J., & McConnell, H. M. (1972) *Chem. Phys. Lett. 13*, 115.

McGaffney, B. J. (1979) *J. Phys. Chem. 83*, 3345.

McGhee, J. D., & von Hippel, P. H. (1974) *J. Mol. Biol. 80*, 469.

McGhee, J. D., & Felsenfeld, G. (1980) *Annu. Rev. Biochem. 49*, 1115.

Millar, D. P., Robbins, R. J., & Zewail, A. H. (1980) *Proc. Natl. Acad. Sci. U.S.A. 77*, 5593.

Miller, K. J. (1979) *Biopolymers 18*, 959.

Noll, M., Thomas, J. O., & Kornberg, R. O. (1975) *Science (Washington, D.C.) 187*, 1203.

Olins, A. L., & Olins, D. E. (1979) *J. Cell Biol. 81*, 266.

Paoletti, J., Magee, B. B., & Magee, P. T. (1977) *Biochemistry 16*, 351.

Pulleyblank, D. E., Shore, M., Tang, D., Vinograd, J., & Vosberg, H. P. (1975) *Proc. Natl. Acad. Sci. U.S.A. 72*, 4280.

Robinson, B. H., & Dalton, L. R. (1980) *J. Chem. Phys. 72*, 1312.

Robinson, B. H., Hurley, I., Scholes, C. P., & Lerman, L. S. (1979) in *Stereodynamics of Molecular Systems* (Sarma, R. H., Ed.) Pergamon Press, New York.

Robinson, B. H., Lerman, L. S., Beth, A. H., Frisch, H. L., Dalton, L. R., & Auer, C. (1980a) *J. Mol. Biol. 139*, 13.

Robinson, B. H., Forgacs, G., Dalton, L. R., & Frisch, H. L. (1980b) *J. Chem. Phys. 73*, 4688.

Rozantzev, E. G. (1970) *Free Nitroxyl Radicals*, Plenum Press, New York.

Shore, J. E., & Zwanzig, R. (1975) *J. Chem. Phys. 63*, 5445.

Thomas, D. D., Dalton, L. R., & Hyde, J. S. (1976) *J. Chem. Phys. 65*, 3506.

Wahl, P., Paoletti, C., & LePecq, J. B. (1970) *Proc. Natl. Acad. Sci. U.S.A. 65*, 417.

Wakelin, L. P. G., & Waring, M. J. (1974) *Mol. Pharmacol. 9*, 544.

Wakelin, L. P. G., & Waring, M. J. (1980) *J. Mol. Biol. 144*, 183.

Waring, M. (1976) *J. Mol. Biol. 54*, 247.